Low-temperature X-ray diffraction, transport properties, specific-heat, thermal expansion and magnetic investigations of $SmCu_2$

1990 J. Phys.: Condens. Matter 2 1485

(http://iopscience.iop.org/0953-8984/2/6/008)

J. Phys.: Condens. Matter **2** (1990) 1485–1498. Printed in the UK

Low-temperature x-ray diffraction, transport properties, specific-heat, thermal expansion and magnetic investigations of $SmCu_2$

E Gratz†, N Pillmayr†, E Bauer†, H Müller†, B Barbara‡ and M Loewenhaupt§

† Institut für Experimentalphysik, Technical University of Vienna, Wiedner Hauptstrasse 8–10, A-1040 Vienna, Austria

‡ Laboratoire Louis Néel, CNRS Grenoble, F-38042 Grenoble, France

§ Institut für Festkörperforschung, KFA Jülich, D-5170 Jülich, Federal Republic of Germany

Received 7 August 1989, in final form 23 October 1989

Abstract. A variety of physical properties (low-temperature x-ray diffraction, electrical resistivity, thermal conductivity, thermopower, specific heat, thermal expansion and susceptibility) of orthorhombic $SmCu_2$ have been studied. A significant contribution of the $J = \frac{5}{2}$ Hund ground state has been observed. An estimation of the overall crystal-field splitting obtained from the thermal expansion experiment yields a value of 110 K. The magnetic entropy indicates a doublet ground state, since the observed value ($S_m = 5.50 \pm 0.2$ J mol^{-1} K^{-1}) is very near to the theoretical R ln 2. An additional influence of the $J = \frac{7}{2}$ multiplet is visible in the resistivity and susceptibility results. The pronounced increase of the thermal conductivity in the magnetically ordered region (Néel temperature $T_N = 23$ K) is discussed within the framework of magnon-heat conductivity.

1. Introduction

Among the REM_2 compounds (RE = rare-earth element, M = transition metal) the $MgCu_2$ structure exists for all 3d elements M from Mn to Ni. By contrast the intermetallic $RECu_2$ compounds exhibit the orthorhombic $CeCu_2$ type of structure with the space group Imm*a*.

The first magnetic investigations performed on the $RECu_2$ compounds by Sherwood *et al* (1964) revealed an antiferromagnetic structure for most of these compounds. Single-crystal investigations (Hashimoto *et al* 1979a, b) confirmed these results. From neutron diffraction experiments (see, e.g. Lebech *et al* 1987) and specific-heat measurements (Luong *et al* 1985) it has been found that in most of the $RECu_2$ intermetallics one (or more) first- or second-order transitions exist below the Néel temperature T_N, associated with changes in the magnetic structure. The highest ordering temperature within the $RECu_2$ series was found to be $T_N = 54$ K for $TbCu_2$ whereas the lowest currently known is 1000 times smaller for $PrCu_2$ ($T_N = 56$ mK). Summarising these results, the $RECu_2$ compounds show a large variety of magnetic behaviour.

Within the family of the $RECu_2$ compounds $CeCu_2$ has been identified as a Kondo compound (Gratz *et al* 1985). Concerning the crystal-field influence on the different

0953-8984/90/061485 + 14 $03.50

physical properties, it may be expected that in $SmCu_2$ and $EuCu_2$ the higher multiplets have to be considered to some extent. Recently Isikawa *et al* (1988) were able to show that the strong curvature in the inverse susceptibility of $SmCu_2$ is caused by the $J = \frac{7}{2}$ multiplet.

Stimulated by these investigations, we started to extend the study of $SmCu_2$ by applying low-temperature structural investigations, measurements of transport properties, thermal expansion, specific heat and magnetisation, in order to obtain an overview of the physical properties of $SmCu_2$.

2. Sample preparation and experimental techniques

The components of $SmCu_2$, YCu_2 and $LuCu_2$ samples were melted together in a water-cooled copper boat by means of induction heating in a helium atmosphere. The polycrystalline ingots were annealed in an evacuated quartz tube at 700 °C for 72 h. All experiments described below were performed on the same sample.

A Siemens x-ray diffractometer was used to check the phase purity and to measure the lattice parameters a, b and c at room temperature. For the low-temperature x-ray diffraction experiment a He-flow cryostat was mounted on the diffractometer in place of the standard specimen holder. To test the calibration of the diffractometer with the mounted cryostat at any temperature, we have mixed tungsten powder with the $SmCu_2$ powder. For all measurements $CuK\alpha_1$–$K\alpha_2$ radiation has been used. The absolute accuracy of the lattice parameters as obtained by x-ray diffraction with the standard specimen holder is ±0.003 Å. Using the cryostat instead of the standard sample holder the accuracy is lower (see § 3.1).

Transport properties (electrical resistivity ρ, thermal conductivity λ and thermopower S) have been measured from 1.5 K up to about 1000 K with different equipment for the low-temperature (1.5–300 K) and high-temperature (280–1000 K) measurements. The $\rho(T)$ experiments in both temperature regions were carried out by means of a conventional four-probe technique applied to a bar-shaped sample with dimensions $1.5 \times 1.8 \times 12\ mm^3$. The absolute temperature was read from the voltage along thermocouples (Au + 0.07% Fe/chromel at low temperatures; chromel/alumel at high temperatures).

In the thermal conductivity measurement a temperature difference ΔT of the order of 0.3–1 K (low temperature) and 2–20 K (high temperature) was established and measured with differential thermocouples (Au + 0.07% Fe/chromel at low temperature; NiCr/NiAl at high temperature). In the steady-state measuring method, the thermal conductivity is given by

$$\lambda(T) = (\mathrm{d}Q/\mathrm{d}t)l/A\Delta T$$

where $\mathrm{d}Q/\mathrm{d}t$ is the heating power, l the length of the sample and A the cross section of the sample. In the high-temperature experiment we determined Q indirectly by a comparator technique (Laubitz 1969). The reproducibility of the $\rho(T)$ and $\lambda(T)$ data is better than 0.5%, whereas, owing to the uncertainty in the sample geometry, the absolute values of ρ and λ are about ±5% below room temperature. Owing to the influence of thermal radiation above 700 K the uncertainty of the $\lambda(T)$ data increases to about 10%.

The absolute thermopower $S_x(T)$ was calculated from the equation

$$S_x(T) = S_r(T) - U_{rx}/\Delta T.$$

$S_r(T)$ is the absolute thermopower of the reference material (Pb at low temperature and Pt at high temperature), whereas U_{rx} is the thermal induced voltage across the sample and depends on the value of the temperature difference ΔT. To estimate the uncertainty in the absolute value of the thermopower, two different $SmCu_2$ samples have been measured. Both $S(T)$ curves were identical within an error bar of $0.5\ \mu V\ K^{-1}$ in the whole temperature range.

The specific-heat measurements were performed using an adiabatic calorimeter in the temperature range 1.5–60 K. The calorimeter, employing the Nernst method of step heating, was calibrated and tested using high-purity Cu (99.9999%) (Schmitzer 1985). The absolute accuracy is estimated to be better than 1% in the low-temperature range and about 3% for $T > 30$ K.

For the thermal expansion measurements a membrane technique has been used (Grössinger and Müller 1981). The deformation of the Cu–Be membrane is measured with a special strain gauge, which is glued on the membrane. Because of the brittleness of the $RECu_2$ samples, it cannot be excluded that there are microcracks in our spherical-shaped samples used for the thermal expansion experiment. The estimated error in $\alpha(T)$ is about 10%.

The DC susceptibility has been obtained by the induction method in a magnetometer within a superconducting coil (0–70 kOe) and a helium-flow temperature regulation (±0.01 K between 1.5 and 300 K).

3. Results and discussion

3.1. Structural investigation

As already mentioned in the introduction, among the RE–Cu compounds the members of the family of $RECu_2$ crystallise in the orthorhombic $CeCu_2$ structure, which belongs to the space group Imm*a* (Storm and Benson 1963) except $LaCu_2$ (hexagonal AlB_2 type). Figure 1 shows our lattice parameter results obtained for all $RECu_2$ compounds. The lattice parameters of $EuCu_2$ and $YbCu_2$ are anomalously large compared to the other $RECu_2$ compounds, pointing to an intermediate valence between 3+ and 2+ for these two RE ions. The lattice parameters of $SmCu_2$ ($a = 4.362 \pm 0.002$ Å, $b = 6.932 \pm 0.003$ Å, $c = 7.368 \pm 0.003$ Å) measured at 290 K fit well into the general behaviour of the trivalent $RECu_2$ compounds. Within the experimental accuracy of these experiments we deduced a valence of the Sm ion in $SmCu_2$ close to 3. We obtained the lattice constants by monitoring the (0 2 2), (1 2 1), (1 1 2), (2 0 0), (1 0 3) and (2 2 2) Bragg reflections by step scanning. A step width of 0.02° in 2θ has been used. The exact 2θ position of the corresponding $K\alpha_1$ or $K\alpha_2$ line has been obtained from fits of Lorentzian functions to the experimental data. As an example figure 2 shows the results of such a fit procedure to the copper $K\alpha_1$–$K\alpha_2$ doublets of the (0 2 2), (1 2 1) and (1 1 2) reflections. This analysis was also applied to obtain the temperature dependence of the lattice parameters at low temperatures. Figure 3 shows the temperature dependence of the lattice parameters *a*, *b* and *c* and the volume of the unit cell. A kink in the temperature variation near 23 K corresponds to the magnetic ordering temperature. It is notable that the lattice parameters *a* and *c* only show a weak temperature dependence in the region

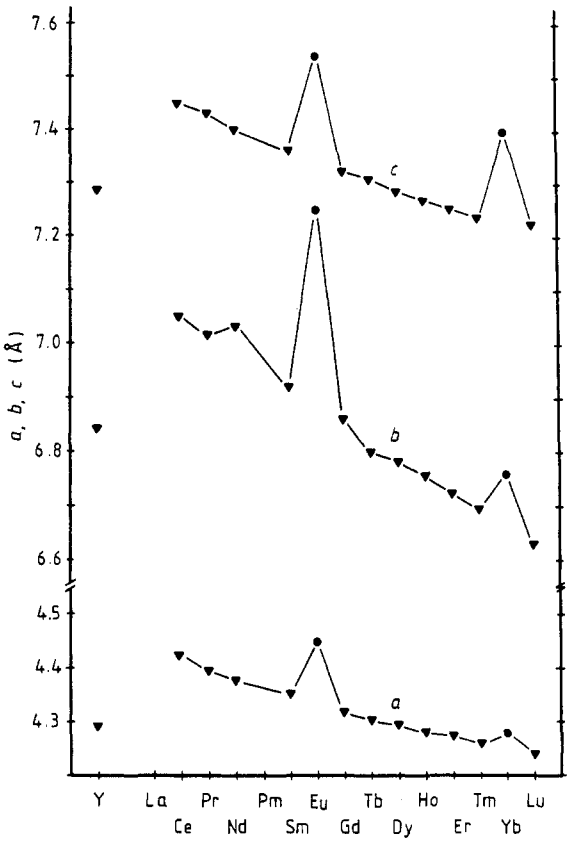

Figure 1. Orthorhombic lattice parameters a, b and c versus the atomic numbers of the $RECu_2$ compounds. The larger a, b and c values for $EuCu_2$ and $YbCu_2$ arise from the intermediate valence state of the Eu and Yb ions. (The error bars are of the size of the symbols.)

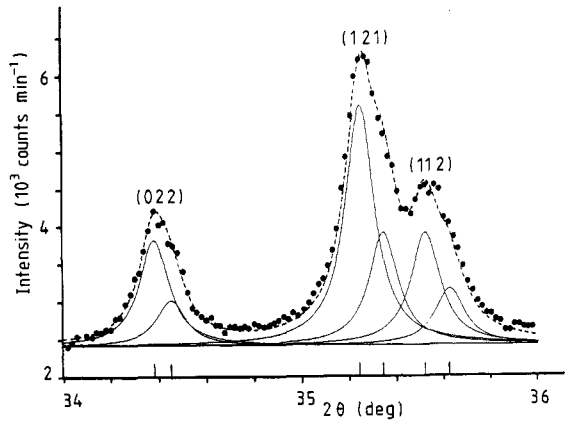

Figure 2. X-ray line profile of the (0 2 2), (1 2 1) and (1 1 2) reflections. The centre of gravity of the Lorentzian function fitted to the experimental data (given as full curves) is taken as the 2θ value for the corresponding $K\alpha_1$ or $K\alpha_2$ reflection.

from 4.2 K to room temperature. Although the uncertainty in the determination of b is larger compared to $a(T)$ or $c(T)$, it clearly follows that b versus T exhibits a much larger temperature dependence, accompanied by a pronounced negative curvature around 100 K. Borombaev *et al* (1987) also observed a considerably larger temperature variation of the b lattice constant for the isostructural $GdCu_2$ compound, but without observing

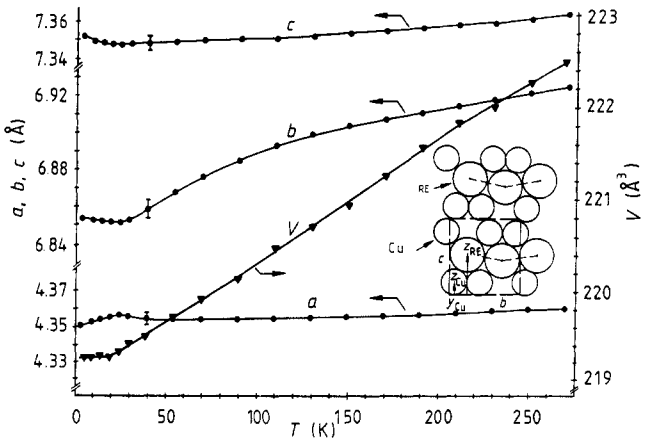

Figure 3. Temperature dependence of the lattice parameters a, b and c and the volume V of the unit cell. Note the much stronger variation of the b axis with temperature. The inset shows the bc plane of the $CeCu_2$ type of structure with parallel zig-zag chains of Sm atoms.

the negative curvature. Since there is no crystal-field influence in $GdCu_2$ the curvature in $b(T)$ around 100 K in $SmCu_2$ is caused by the crystal field, in agreement with what has been found from other experiments (see §§ 3.2.1 and 3.4). Considering the atomic arrangement of the Sm and Cu atoms in the unit cell of the $CeCu_2$ structure, one realises that the strong temperature dependence of the lattice parameter in the b direction is closely connected with the atomic arrangement of the Sm atoms in this direction. The inset in figure 3 shows the bc plane of the $CeCu_2$-type structure, which is built up by layers in the sequence ABAB . . . along the a axis. In each layer the Sm atoms form parallel zig-zag chains, which are separated by Cu atoms. In order to explain the strong thermal variation of the b lattice parameter with decreasing temperature, it might be assumed that either the amplitude of the zig-zag arrangement increases or the diameter of the Sm ions decreases on lowering the temperature. The latter case would indicate a variation of the valence of the Sm ion at lower temperatures. However, the results from other experiments (see below in § 3.5) reveal that such an explanation is rather unlikely. It should also be mentioned that for the various $RECu_2$ compounds the reduction of the b axis due to the lanthanide contraction is considerably larger (6.33%) than that of the a axis (3.8%) or the c axis (3.5%) (see figure 1). Since the a and c lattice parameters are mainly determined by the Cu–Cu distances, this effect is certainly due to the fact that RE chains exist along the b direction.

3.2. Transport properties

3.2.1. Electrical resistivity. The temperature dependence of the electrical resistivity $\rho(T)$ of $SmCu_2$ is given in figure 4. The curve is characterised by a sharp kink at the magnetic ordering temperature T_N (see also the inset). A further small step in ρ versus T near 17 K points to an additional magnetic transition. Changes in the magnetic structure are known to exist in other $RECu_2$ compounds, e.g. $HoCu_2$ (Gratz and Zuckermann 1982) or $ErCu_2$ (Franse *et al* 1985). Another interesting feature is the strong negative curvature of $\rho(T)$; the curvature in ρ versus T starting at 50 K is caused by the split $J = \frac{5}{2}$ multiplet due to the crystal-field influence. At high temperatures the curvature of $\rho(T)$ is mainly due to band-structure effects. In a theoretical investigation (Brunner 1989) it could be shown that the Fermi smearing effect can cause a pronounced negative curvature as long as the Fermi energy is situated near to the bottom of a sharp minimum.

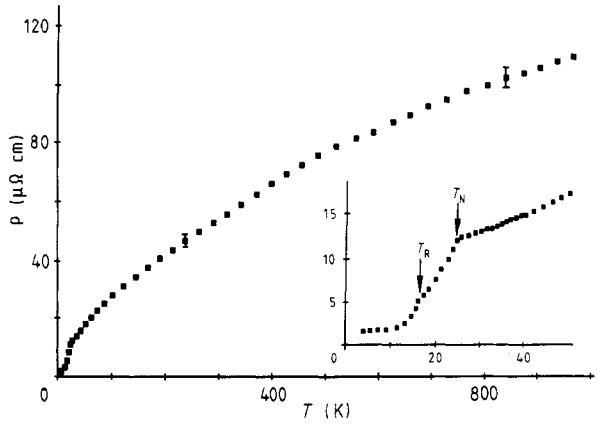

Figure 4. Temperature dependence of the electrical resistivity ρ of $SmCu_2$ from 4.2 up to 1000 K. The inset shows details of ρ versus T at T_N (=23 K) and at the spin-reorientation temperature T_R (=17 K).

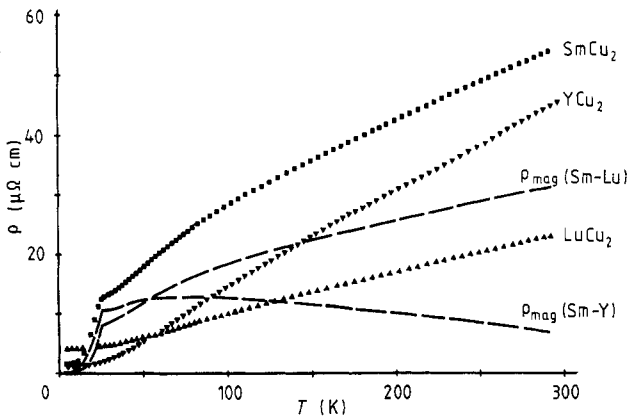

Figure 5. Temperature dependence of the electrical resistivity ρ of the isostructural compounds $SmCu_2$ (magnetic) and YCu_2 and $LuCu_2$ (non-magnetic) in the range 4.2 up to 280 K. After subtracting the residual resistivities ρ_0 the magnetic contribution $\rho_{mag}(Sm - Lu)$ was obtained from $\rho(SmCu_2) - \rho(LuCu_2)$; likewise $\rho_{mag}(Sm - Y) = \rho(SmCu_2) - \rho(YCu_2)$.

This assumption can also explain the sign and the shape of the thermopower at higher temperatures (see § 3.2.3).

The magnetic contribution to the resistivity ρ_{mag} has been obtained by assuming that Matthiessen's rule can be applied:

$$\rho(T) = \rho_0 + \rho_{ph}(T) + \rho_{mag}(T). \tag{3.1}$$

A residual resistivity of 1.3 $\mu\Omega$ cm has been measured for our $SmCu_2$ sample. In principle the phonon contribution $\rho_{ph}(T)$ can be deduced from the resistivity measured for the isostructural non-magnetic YCu_2 or $LuCu_2$. However, as shown in figure 5, $\rho(YCu_2)$ and $\rho(LuCu_2)$ differ considerably; in fact this is not very surprising, since inelastic neutron scattering experiments (Loewenhaupt 1989) recently performed on YCu_2, $CeCu_2$, $PrCu_2$ and $NdCu_2$ show that the phonon spectra are shifted to higher frequencies for YCu_2 compared to the other $RECu_2$, as expected from the lower masses in YCu_2. $LuCu_2$ seems to be more appropriate than YCu_2 for the determination of ρ_{ph} since the

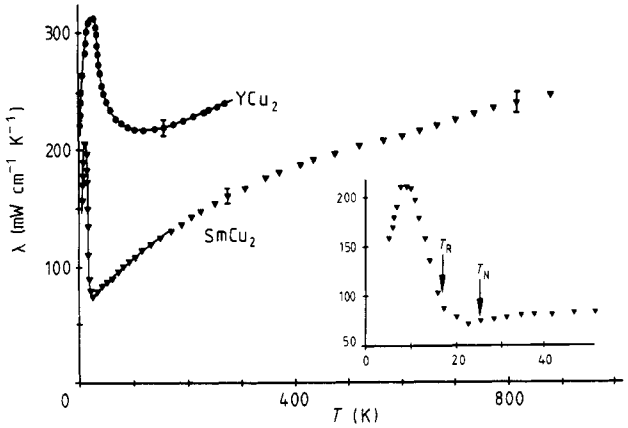

Figure 6. Temperature dependence of the thermal conductivity λ of $SmCu_2$ (4.2 to 900 K) and YCu_2 (4.2 to 300 K). The inset shows the low-temperature maximum in more detail (T_N is the Néel temperature and T_R is the spin-reorientation temperature).

atomic properties of Lu (especially the atomic mass) are much closer to those of Sm, Ce, Pr and Nd. In figure 5, $\rho_{mag}(Sm - Lu)$ and $\rho_{mag}(Sm - Y)$ are depicted as a function of temperature; the former has been obtained by subtracting $\rho(LuCu_2)$ and the latter by subtracting $\rho(YCu_2)$. The behaviour of $\rho_{mag}(Sm - Lu)$ looks normal, while the decrease of $\rho_{mag}(Sm - Y)$ at higher temperatures seems unphysical, at least for a non-Kondo system.

The steep increase of ρ_{mag} above T_N, followed by pronounced curvature, is obviously caused by a crystal-field splitting (Fulde 1978, Gómez-Sal *et al* 1986). An estimation of the overall crystal-field splitting obtained from thermal expansion (see § 3.4) reveals a value of 110 K for $SmCu_2$. The linear increase of $\rho_{mag}(Sm - Lu)$ above 100 K is either due to the fact that the subtracted ρ_{ph} taken from $LuCu_2$ is not really the same as in $SmCu_2$ or, which is much more likely, due to the influence of the higher multiplet $J = \frac{7}{2}$ (see § 3.5). In cases where the crystal-field influence is negligible, ρ_{mag} becomes temperature-independent above T_N; this behaviour has been observed for the heavy $REAl_2$ compounds (Gratz 1988).

3.2.2. Thermal conductivity. The temperature dependence of the thermal conductivity of $SmCu_2$ in the range from 4.2 up to 900 K is depicted in figure 6. The inset shows details below the magnetic ordering temperature (T_N and the spin-reorientation temperature T_R are indicated by arrows). Certainly the most remarkable feature of this λ versus T curve is the pronounced increase of $\lambda(T)$ below T_R. This observation is quite in contrast to the behaviour of $\lambda(T)$ for the other magnetic $RECu_2$ compounds that we have studied up to now. The $\lambda(T)$ curves of $HoCu_2$, $DyCu_2$, $ErCu_2$ and $TmCu_2$ in general show a smooth minimum at the magnetic ordering temperatures and at their spin-reorientation temperatures. In this connection it should be mentioned that in two compounds in the $REAl_2$ family ($PrAl_2$ and $NdAl_2$) pronounced maxima in $\lambda(T)$ below the magnetic ordering temperatures have been observed (Bauer *et al* 1986). Maxima in λ versus T at low temperatures are sometimes observed for pure metals (Parrot and Stuckes 1975) and in non-magnetic compounds as long as their residual thermal resistivity is low enough; for example, we found a maximum in λ versus T for YCu_2 but not for $LuCu_2$. For comparison we included the shape of the $\lambda(T)$ curve of YCu_2 below room temperature in figure 6. There is qualitatively a striking difference between both $\lambda(T)$ curves: the

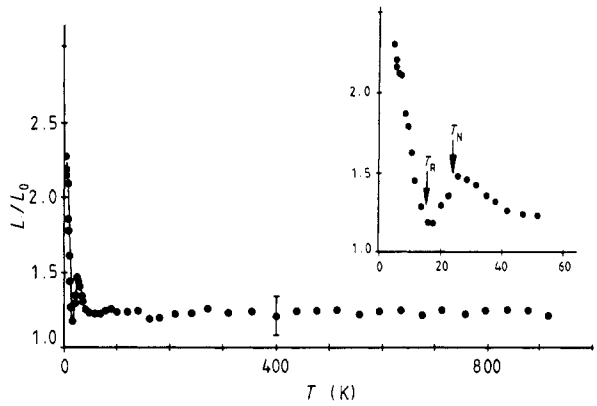

Figure 7. Temperature variation of the normalised Lorenz number $L(T)/L_0 (L_0 = 2.45 \times 10^{-8} \text{V}^2\text{K}^{-2})$ in the range from 4.2 up to 900 K.

maximum in $\lambda(T)$ of $SmCu_2$ is limited to temperatures below T_R. We therefore conclude that the reason for the increase is of magnetic origin, which will now be discussed.

In general the heat transport within a magnetic ordered material can be caused by three components, the electrons, the phonons and also a magnetic component, where the collective spin excitations (magnons) are considered to be the heat carriers. Thus the total thermal conductivity is given by

$$\lambda(T) = \lambda_e(T) + \lambda_{ph}(T) + \lambda_{mag}(T) \tag{3.2}$$

with λ_e the electronic, λ_{ph} the phonon and λ_{mag} the magnetic contributions; generally λ_e is the dominant term. If we assume that the magnons can carry heat described by a large λ_{mag} contribution, the maximum in λ versus T at 10 K can be understood.

A further indication for the importance of magnon-heat transport can be obtained by considering the temperature dependence of the Lorenz number

$$L(T) = \rho(T)\lambda(T)/T.$$

The conditions under which $L(T)$ becomes temperature-independent

$$L(T) = L_0 = 2.45 \times 10^{-8}\ \text{V}^2\ \text{K}^{-2}$$

according to the Wiedemann–Franz law are:

(i) λ_{ph} and λ_{mag} are negligible in equation (3.2) and
(ii) the relaxation-time approximation is valid.

Generally $L(T)/L_0$ (normalised Lorenz number) at low temperatures (where the impurity scattering processes dominate) becomes equal to 1, but in cases where the thermal conductivity is strongly influenced by magnon conductivity $L(T)/L_0$ increases.

$L(T)/L_0$ versus T is plotted in figure 7. Indeed we observe a steep increase below T_R. However, an open question still remains: Why are the magnons so effectively involved in heat transport processes only in some $RECu_2$ or $REAl_2$ compounds? The normalised Lorenz number is also shown as hardly temperature-dependent in the range above T_N up to the highest temperatures available.

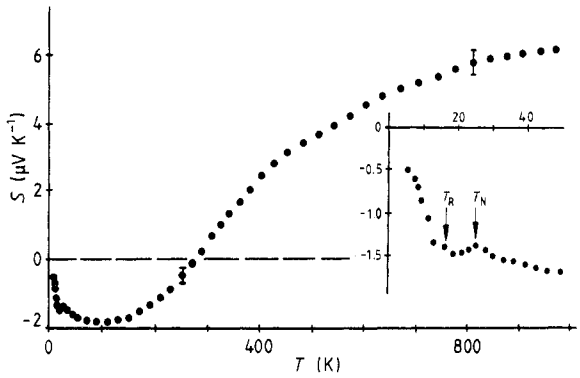

Figure 8. Temperature dependence of the thermopower S of $SmCu_2$ in the range from 4.2 up to 1000 K. The inset shows details of S versus T below 50 K.

3.2.3. Thermopower. The thermopower $S(T)$ is presented in figure 8. The inset shows details of $S(T)$ below 40 K. Instead of Matthiessen's rule, in the case of thermopower the Nordheim–Gorter rule has to be used when taking into account different scattering processes (Gratz and Nowotny 1985):

$$S(T) = (\rho_0/\rho)S_0(T) + (\rho_{ph}/\rho)S_{ph}(T) + (\rho_{mag}/\rho)S_{mag}(T). \tag{3.3}$$

In principle this rule represents a possibility for the separation of the different scattering contributions caused by potential scattering, phonon scattering and spin-dependent scattering processes (Gratz 1981). Systematic measurements of the temperature dependence of the thermopower of all the $RECu_2$ compounds below room temperature clearly show that spin-dependent scattering influences the total thermopower in a characteristic way (Gratz and Zuckermann 1982). Various theoretical calculations also confirm that crystal-field effects should be visible in S versus T. For example Fulde (1978) could show that a crystal-field splitting can give rise to a maximum or minimum in $S(T)$. In the case of $SmCu_2$ the crystal-field influence on the thermopower is difficult to determine. On the other hand it is known that the sign and the curvature of S versus T especially at high temperatures depend sensitively on the details of the density-of-states function near the Fermi energy. In our very recent theoretical investigations we could show that the shape of $S(T)$ observed for $SmCu_2$ (see figure 8) can be understood if the Fermi energy is situated on the left-hand side of a deep minimum in $N(\varepsilon)$ (Brunner 1989). Coming back to the crystal-field influence on $S(T)$, a tentative estimation yields that the broad minimum around 100 K is at least partly caused by the crystal field.

3.3. Specific heat

Figure 9 shows the temperature dependence of the specific heat C_p and the magnetic contribution S_m to the total entropy. The magnetic phase transition temperature T_N (= 23 K) and the spin-reorientation temperature (T_R = 17 K) are characterised by second-order-type peaks in C_p versus T. In contrast to Isikawa *et al* (1988) we do not observe a third anomaly around 9 K. The temperature-dependent behaviour of $C_p(T)$ of $SmCu_2$ can be described by the common expression

$$C_p(T) = \gamma T + \beta T^3 + C_{mag}(T) + C_{nucl}(T) \tag{3.4}$$

with γT the electronic and βT^3 the phonon contributions to the specific heat. C_{mag}

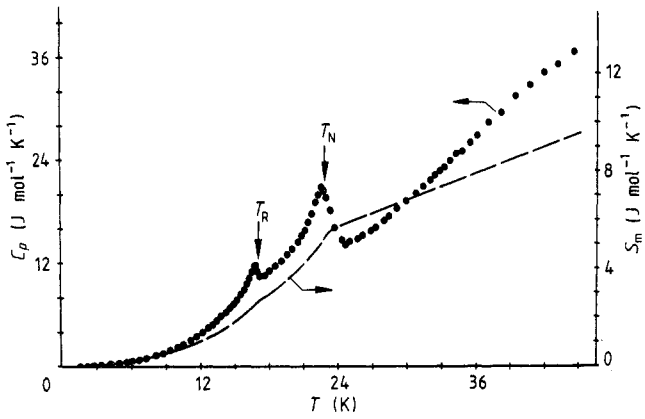

Figure 9. Temperature dependence of the specific heat C_p and the magnetic entropy S_m of $SmCu_2$ from 1.5 up to 45 K.

represents the magnetic and C_{nucl} the nuclear contributions. For antiferromagnetic spin waves the magnetic term is given by the expression $C_{mag} = \delta T^3$.

From the C_p/T versus T^2 plot the γ coefficient was estimated to be about 20 mJ mol^{-1} K^{-2}. This value is about twice as high as the γ values observed for the other $RECu_2$ compounds, e.g. $\gamma(TmCu_2) = 9$ mJ mol^{-1} K^{-2} (Šima *et al* 1988) and $\gamma(YCu_2) = 6.7$ mJ mol^{-1} K^{-2} (Luong *et al* 1985). However, the γ value for $SmCu_2$ is four times smaller than that observed for the isostructural Kondo system $CeCu_2$, $\gamma(CeCu_2) = 82$ mJ mol^{-1} K^{-2} (Gratz *et al* 1985).

The change of the magnetic entropy up to T_N was obtained from

$$S_m = \int_0^{T_N} C_{mag}/T \, dT. \tag{3.5}$$

For the determination of C_{mag} the phonon contribution C_{ph} has been obtained from the non-magnetic isostructural $LuCu_2$: $C_{mag} = C_p(SmCu_2) - C_p(LuCu_2)$ (as already discussed in § 3.2.1, $LuCu_2$ is more appropriate than YCu_2). Thus, the value of S_m obtained for $SmCu_2$ is 5.50 ± 0.2 J mol^{-1} K^{-1}, very near to the value expected for complete removal of the two-fold spin degeneracy of a crystal-field ground-state doublet ($S_m = R \ln 2 = 5.76$ J mol^{-1} K^{-1}). Isikawa *et al* (1988) observed an S_m value that is 0.88 of the theoretical value. We conclude from the C_p experiment that the ground state is a doublet. The $J = \frac{5}{2}$ multiplet of S is split into three doublets in this orthorhombic structure. The steep increase of $S_m(T)$ above T_N points to the existence of another doublet not far away from the ground-state doublet.

3.4. Thermal expansion

Since our specific-heat equipment does not allow us to reach temperatures high enough to observe the Schottky anomaly caused by higher excited doublets, we performed thermal expansion measurements in the range from 4 K up to room temperature. For $SmCu_2$ the coefficient of thermal expansion $\alpha = d(\Delta l/l)/dT$ is given in figure 10. Also $\alpha(T)$ of the isostructural $LuCu_2$ compound is shown in this figure, too. For the analysis of the $\alpha(T)$ data of $SmCu_2$ in the paramagnetic temperature range, we used

$$\alpha(T) = \alpha_e(T) + \alpha_{ph}(T) + \alpha_{mag}(T). \tag{3.6}$$

The first term represents the electronic contribution, the second one the phonon part

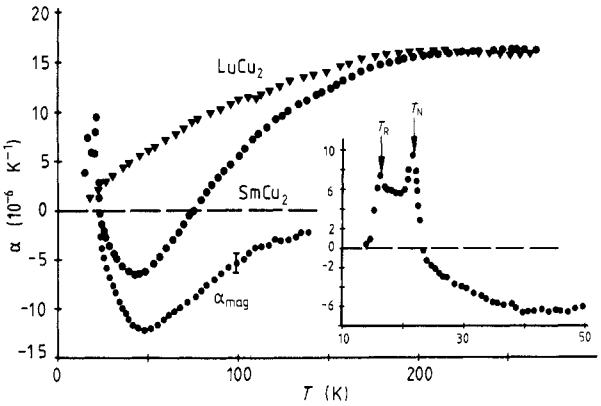

Figure 10. Temperature dependence of the thermal expansion α of $SmCu_2$ and $LuCu_2$ and the magnetic contribution α_{mag} to the thermal expansion. The inset shows details of α versus T below 50 K.

and α_{mag} is the spin-dependent induced thermal expansion. Comparing $\alpha(T)$ of $LuCu_2$ with $\alpha(T)$ of $SmCu_2$ it is striking that $\alpha(T)$ of $SmCu_2$ shows a pronounced minimum near 40 K, which does not appear in $LuCu_2$ or YCu_2; $\alpha(T)$ of YCu_2 has also been measured but is not shown in figure 10.

From previous investigations of $\alpha(T)$ on $ErCu_2$ (Franse *et al* 1985) and $TmCu_2$ (Šima *et al* 1988) it follows that the crystal-field influence on the thermal expansion can cause a minimum in α_{mag} (as long as the ordering temperature is low enough). We therefore determined $\alpha_{mag}(T)$ for $SmCu_2$ by subtracting $\alpha(T)$ of the isostructural non-magnetic $LuCu_2$ compound. Figure 10 shows $\alpha_{mag}(T)$ of $SmCu_2$ with a minimum at 45 K. Assuming that the minimum in $\alpha_{mag}(T)$ represents an effect comparable to the Schottky-type anomaly in the specific heat, the position of the minimum temperature (T_m = 45 K) can be used to estimate roughly the splitting between the ground-state doublet and the first excited doublet. This is based on the following assumptions:

(i) $\alpha_{mag} = AC_{mag}$ shows the same temperature dependence as the specific heat C_{mag} (A being weakly dependent on temperature).

(ii) In a two-level system (here two doublets) the specific heat attains a maximum value at an intermediate temperature T_m given by (Gopal 1966):

$$(g_0/g_1)\exp(\delta/T_m) = [(\delta/T_m) + 2]/[(\delta/T_m) - 2]. \tag{3.7}$$

If the separation between the two higher doublets were of the order of or larger than δ, then $g_0/g_1 = 1$ (g_0 and g_1 denote the degeneracies of the two lowest levels). In this case the maximum occurs at $T_m = 0.42\delta$, where $\delta = \varepsilon/k_B$ (energy separation measured in kelvins).

As a result we obtained for the distance between the ground-state doublet and the next higher level a value of about 110 K. If the two excited doublets were much closer in energy than δ, then $g_0 = 2$ and $g_1 = 4$; we find $\delta \cong 100$ K, not very different from the preceding case. In fact other implicit assumptions such as the isotropy of the system are much more questionable; nevertheless we believe that the order of magnitude is quite sufficient.

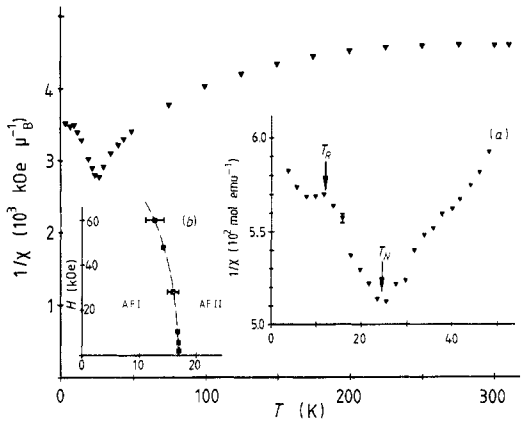

Figure 11. Temperature dependence of the inverse susceptibility χ^{-1}. Inset (*a*) shows details around the Néel temperature T_N and the spin-reorientation temperature T_R (at 60 kOe). Inset (*b*) gives the field dependence of T_R (AFI and AFII denote different antiferromagnetic structures).

3.5. Magnetic measurements

Up to 60 kOe the magnetisation of $SmCu_2$ varies linearly with the applied field at any temperature. The deduced susceptibility, plotted in figure 11 versus the temperature, shows a well defined cusp at the Néel temperature $T_N = 23$ K and a rapid saturation towards a constant value χ_0 at higher temperatures. The experimental data were fitted to the common form

$$\chi = C/(T + \theta_p) + \chi_0 \tag{3.8}$$

with the obtained parameters $\chi_0 = 1.07 \times 10^{-3}$ emu mol^{-1}, $C = 3.53 \times 10^{-2}$ emu K mol^{-1} and $\theta_p = -14$ K. As in many other Sm-based systems the constant contribution χ_0 arises from the contribution of the excited $J = \frac{7}{2}$ multiplet. From the Curie constant C an effective paramagnetic moment $\mu_{eff} = 0.53\mu_B$ has been determined, which is in good agreement with the value obtained for other Sm-based systems (de Wijn *et al* 1976). The paramagnetic temperature $\theta_p = -14$ K shows that negative interactions are predominant. The inset in figure 11(*a*) shows details of the susceptibility around the Néel temperature. A second anomaly is observed between 12 and 17 K (depending on the applied field), which is certainly connected with the specific-heat, resistivity and thermal expansion anomalies found at 17 K.

We have no direct indications for the origin of this transition; however, below T_N most other compounds of the $RECu_2$ series show one (or more) first- or second-order transitions associated with changes in the magnetic structure. The field dependence of this spin-reorientation temperature T_R is given in the inset in figure 11(*b*) (AFI and AFII denote different types of antiferromagnetic spin arrangements). No field dependence of T_N was observed for fields up to 60 kOe.

The linear dependence of M versus H is not surprising since the metamagnetic field should be of the order of 40 T. In fact a critical field of 22 T in the *b* direction of a single crystal has been obtained (Maezawa *et al* 1989).

4. Summary

The conclusions of the present paper can be summarised as follows:

A comparison of the lattice constants (orthorhombic $CeCu_2$ structure) in the series of the $RECu_2$ compounds reveals that the Sm ion is in the 3+ state. Of the three parameters a, b and c, b shows a much stronger dependence on temperature than do the other two. This has been attributed to the fact that chains of RE atoms exist in the b direction. The 'zig-zag' arrangement of the RE atoms becomes rearranged on cooling down, giving rise to the much stronger temperature variation in the b axis.

The curvature of the spin-dependent resistivity contribution ρ_{spd} indicates the crystal-field influence on the $J = \frac{5}{2}$ ground state. The open question in that context is the effect of the $J = \frac{7}{2}$ multiplet on ρ_{spd}. From the shape of the high-temperature thermopower behaviour, we conclude that the Fermi energy is situated on the left-hand side of a minimum in the density-of-states function. The drastic increase of the thermal conductivity in the magnetically ordered range below the spin-reorientation temperature is probably caused by magnons, which are responsible for the additional heat transport. Further measurements are needed to confirm this assumption.

The magnetic entropy as deduced from the specific heat at the magnetic ordering temperature is in agreement with the theoretical value $R \ln 2$, indicating a doublet ground state. An analysis of the thermal expansion data indicates a crystal-field splitting between the ground state and the next higher level of about 100 K. As in many other Sm compounds a very strong curvature of the inverse susceptibility is observable, which is frequently attributed to the influence of higher-order multiplets.

Acknowledgments

Part of this work (transport properties) was supported by the Austrian Science Foundation ('Fonds zur Förderung der wissenschaftlichen Forschung in Österreich') under project number P 5883.

We also thank the 'Hochschuljubiläumsstiftung der Stadt Wien' for financial support.

NP expresses his gratitude to the 'Jubiläumsfonds der Österreichischen Nationalbank' under project number 3492.

References

Bauer E, Gratz E and Adam G 1986 *J. Phys. F: Met. Phys.* **16** 493

Borombaev M K, Levitin R Z, Markosyan A S, Reimer A S, Sinitsyn E V and Smetana Z 1987 *Sov. Phys.–JETP* **66** 866

Brunner H 1989 *PhD Thesis* Technical University of Vienna

de Wijn H W, van Diepen A M and Buschow K H J 1976 *Phys. Status Solidi* **76** 11

Franse J J M, Luong N H and Hien T D 1985 *J. Magn. Magn. Mater.* **52** 202

Fulde P 1978 *J. Appl. Phys.* **49** 1311

Gómez-Sal J C, Rodríguez Fernández J, López Sánchez R J and Gignoux D 1986 *Solid State Commun.* **59** 771

Gopal E S R 1966 *Specific Heats at Low Temperatures* ed. K Mendelssohn and K D Timmerhaus (New York: Plenum) ch 4

Gratz E 1981 *J. Magn. Magn. Mater.* **24** 1

—— 1988 *Physica* B **149** 283

Gratz E, Bauer E, Barbara B, Zemirli S, Steglich F, Bredl C D and Lieke W 1985 *J. Phys. F: Met. Phys.* **15** 1975

Gratz E and Nowotny H 1985 *Physica* B **130** 75

Gratz E and Zuckermann M J 1982 *Handbook of the Physics and Chemistry of Rare Earths* ed. K A Gschneidner Jr and L Eyring (Amsterdam: North-Holland) ch 42

Grössinger R and Müller H 1981 *Rev. Sci. Instrum.* **52** 1528

Hashimoto Y, Fujii H, Fujiwara H and Okamoto T 1979a *J. Phys. Soc. Japan* **47** 67
—— 1979b *J. Phys. Soc. Japan* **47** 73
Isikawa Y, Mori K, Takeda H, Umehara I, Sato K, Onuki Y and Komatsubara T 1988 *J. Magn. Magn. Mater.* **76/77** 161
Laubitz H J 1969 *Thermal Conductivity* ed. R P Tye (London: Academic) ch. 3
Lebech B, Smetana Z and Šima V 1987 *J. Magn. Magn. Mater.* **70** 97
Loewenhaupt M 1989 to be published
Luong N H, Franse J J M and Hien T D 1985 *J. Magn. Magn. Mater.* **50** 153
Maezawa K, Wakabayashi S, Sato K, Isikawa Y, Kaneko T, Kido G and Nakagawa Y 1989 *Physica* B **155** 276
Parrot J E and Stuckes A D 1975 *Thermal Conductivity of Solids* ed. J E Parrot (London: Academic) ch 4
Schmitzer C 1985 *PhD Thesis* Technical University of Vienna
Sherwood R C, Williams H J and Wernick J H 1964 *J. Appl. Phys.* **35** 1049
Šima V, Smetana Z, Diviš M, Svoboda P, Zajac Š, Bischof J, Lebech B and Kayzel F 1988 *J. Physique Coll.* **49** (C8) 415
Storm A R and Benson K E 1963 *Acta Crystallogr.* **16** 701